

Transition metal saccharide chemistry and biology: Synthesis, characterization, electrochemistry and EPR studies of oxovanadium(IV) complexes of saccharides and their derivatives and in vitro interaction of some of these with ribonuclease and deoxyribonuclease

Alavattam Sreedhara^a, Chebrolu P. Rao^{a,*}, Basuthkar J. Rao^b

^a *Bioinorganic Laboratory, Department of Chemistry, Indian Institute of Technology, Powai, Bombay 400 076, India*

^b *Molecular Biology Unit, Tata Institute of Fundamental Research, Homi Bhabha Road, Bombay 400 005, India*

Received 25 October 1995; accepted 25 March 1996

Abstract

Low molecular weight, water-soluble saccharide complexes of oxovanadium(IV) have been synthesized and characterized by analytical, spectroscopic and electrochemical techniques. All the complexes were found to be mononuclear, possessing the VO^{2+} moiety. These are shown to be hydrolytically and oxidatively stable over a wide range of pH (1–12) and have been extensively characterized by absorption and EPR spectroscopy and by electrochemistry. Several correlations have been drawn from the data generated. Some of these complexes have been demonstrated to possess in vitro RNase inhibition activity with no effect on DNase. This suggests that these molecules closely mimic the substrate portion of the RNase-catalysed RNA hydrolysis and can act as transition-state analogues to RNase. © 1996 Elsevier Science Ltd.

Keywords: Transition metal–saccharide chemistry; Oxovanadium(IV)–saccharide complexes; In vitro RNase inhibition; Transition-state analogues; Hydrolytic stability

* Corresponding author. E-mail: cprao@ether.chem.iitb.ernet.in.

1. Introduction

Saccharides and their derivatives are widespread in nature, and their role in various biological activities is recognised. The elucidation of the interactions between metals and saccharides has been a topic of recent interest, mainly due to their roles in enantioselective catalysis, biotechnology, pharmacology, etc. [1]. The inhibitory [2] and promotory [3] roles played by vanadium in its various oxidation states and coordination forms in biological systems is beginning to be understood in the literature.

The isolation of vanadobin, a pale green, low molecular weight compound containing a reducing sugar [4], as the vanadium-binding substance provides additional impetus for the study of the interactions between vanadium and saccharides. There has been great interest in developing soluble and orally active insulin mimetic vanadyl compounds [5]. Insulin-like activity has been demonstrated for some peroxovanadium(V) compounds [6], a bismaltolato vanadyl compound [7], and a dithiocarbamate compound of vanadyl [8]. The isolation of RNA from most animal cells is effected by the inhibition of RNase using a mixture of VOSO_4 and the four ribonucleosides [9]. Recent single-crystal X-ray characterization of $(\text{NEt}_4)_2[\text{VO}_2\text{Ad}]_2$ (where Ad is adenosine) showed that the Ad moiety binds to the cis dioxo-V(V) centre through the 2'- and 3'-hydroxyl groups of the ribose unit [10]. Thus understanding of the various roles played by vanadium certainly demands for the development of its coordination chemistry and biochemistry where saccharide and related molecules act as ligands.

In continuation with our interest in developing the transition metal–saccharide chemistry and biology [11–13], we herein report the synthesis, isolation and characterization of oxovanadium(IV) complexes of pentoses: D-ribose, (VO-D-Rib, **1**); D-xylose, (VO-D-Xyl, **2**); D-lyxose, (VO-D-Lyx, **6**); D-arabinose (VO-D-Ara, **7**); hexose: L-sorbose, (VO-L-Sor, **3**); saccharide derivatives: D-gluconic acid, (VO-D-Gluconate, **8**); D-galacturonic acid, (VO-D-GalA, **4**); Inositol, (VO-Ino, **5**); and L-ascorbic acid, (VO-L-Asc, **9**) and the in vitro interaction of some of these complexes with ribonuclease (RNase) and deoxyribonuclease (DNase).

2. Experimental

Methods and materials.—ESR spectroscopy was performed on a Varian-ESR 112 spectrometer equipped with a low-temperature cavity using tetracyanoethylene (TCNE) as field marker ($g = 2.00277$). ^1H NMR spectra were measured on a Varian XL 300 spectrometer in D_2O . All the complexes were analysed for their C and H content using a Carlo-Erba 1109 analyser, and for their V and Na contents by inductively coupled plasma atomic emission spectroscopy (ICPAES, 8440 Plasma Lab). Cyclic voltammetric experiments were conducted on a BAS100B electrochemical analyser at a hanging mercury drop electrode (HMDE) or a Pt working electrode, in water using an Ag–AgCl reference electrode, Pt wire as auxiliary electrode and NMe_4Cl or NEt_4Br as supporting electrolyte at a scan speed of 100 mV/s. No iR compensation was applied externally.

The pH of the solutions during electrochemical experiments was adjusted using appropriate amounts of 6 N HCl or 10 M NaOH, and pH was monitored using an Elico digital pH meter. Circular dichroism studies were performed in water, using a Jasco 600 spectrophotometer. Room-temperature magnetic moments were measured in the solid state using a Cahn 2000 Faraday balance.

Saccharides and their derivatives and L-ascorbic acid (asc. acid) (Aldrich or Sigma), inositol, acetylacetone (Hacac) (Sisco), sodium metal (Merck) were used as received. RNA Type III, RNase Type IA (EC 3.1.27.5), DNase (EC 3.1.21.1) and Hepes [4-(2-hydroxyethyl)-1-piperazineethane sulfonic acid] buffer were procured from Sigma and were employed in experiments as received. M13RF1 phage DNA was isolated according to literature procedure [14].

Synthesis.—Bis(acetylacetonato)oxovanadium(IV) $[\text{VO}(\text{acac})_2]$ was used as starting material to synthesise the vanadyl–saccharide complexes except **8**, where NH_4VO_3 was used for the synthesis.

$\text{Na}_4[\text{VO}(\text{D-Rib})_2](\text{H}_2\text{O})$ (**1**). To D-Rib (1.50 g, 10 mmol) in 30 mL of MeOH was added freshly cut Na (0.460 g, 20 mmol), and the reaction mixture was stirred for 30 min. To this in situ generated disodium salt of D-ribose was added $\text{VO}(\text{acac})_2$ (1.325 g, 4.98 mmol) in 25 mL of MeOH, dropwise over a period of 30 min. The colour changed from yellow to green, and the reaction was stirred at room temperature for 24 h. A green residue was isolated by filtration and was purified by stirring in hot MeOH at 40 °C for 6 h, followed by a second filtration. This process was repeated thrice before finally isolating the purified green residue and drying in vacuo to give complex **1** in 57% yield. Anal. Calcd for $\text{C}_{10}\text{H}_{14}\text{O}_{11}\text{Na}_4\text{V} \cdot \text{H}_2\text{O}$: C, 25.48; H, 3.39; Na, 19.53; V, 10.81. Found: C, 26.13; H, 3.53; Na, 19.88; V, 10.20%.

$\text{Na}_4[\text{VO}(\text{D-Xyl})_2] \cdot \text{CH}_3\text{OH}$ (**2**). By adopting the procedure given for **1**, complex **2** was isolated in 49% yield. Anal. Calcd for $\text{C}_{10}\text{H}_{16}\text{O}_{11}\text{Na}_4\text{V} \cdot \text{CH}_3\text{OH}$: C, 29.93; H, 4.53; Na, 10.43; V, 11.55. Found: C, 29.93; H, 4.14; Na, 9.87; V, 11.90%.

$\text{Na}_4[\text{VO}(\text{L-Sor})_2] \cdot 3\text{H}_2\text{O}$ (**3**). By adopting the procedure given for **1**, pure complex **3** was obtained in 67% yield. Anal. Calcd for $\text{C}_{12}\text{H}_{18}\text{O}_{13}\text{Na}_4\text{V} \cdot 3\text{H}_2\text{O}$: C, 25.39; H, 4.23; Na, 16.23; V, 8.99. Found: C, 25.49; H, 3.80; Na, 16.70; V, 9.20%.

$\text{Na}_2[\text{VO}(\text{D-GalA})(\text{H}_2\text{O})]$ (**4**). Complex **4** was synthesised and purified following the procedure as given for **1** in 60% yield. Anal. Calcd for $\text{C}_6\text{H}_8\text{O}_9\text{Na}_2\text{V}$: C, 22.43; H, 2.50; Na, 14.33; V, 15.87. Found: C, 22.29; H, 3.10; Na, 14.50; V, 16.00%.

$\text{Na}_2[\text{VO}(\text{Ino})_2]$ (**5**). Complex **5** was synthesised and purified following the procedure explained for **1** to yield 70%. Anal. Calcd for $\text{C}_{12}\text{H}_{20}\text{O}_{13}\text{Na}_2\text{V}$: C, 30.70; H, 4.26; Na, 9.81; V, 10.86. Found: C, 30.04; H, 4.94; Na, 10.03; V, 11.18%.

$\text{Na}_4[\text{VO}(\text{D-Lyx})_2] \cdot 2\text{H}_2\text{O}$ (**6**). To D-Lyx (0.750 g, 5 mmol) in 15 mL MeOH was added freshly cut Na (0.230 g, 10 mmol). $\text{VO}(\text{acac})_2$ (0.665 g, 2.5 mmol) was added as solid, giving a blue–green solution. This was stirred at 40 °C for 24 h. A pale-coloured residue was filtered using Celite, and the filtrate was collected and concentrated and precipitated with acetone to give a green–blue residue. The residue was suspended in EtOH and stirred at 40 °C for 6 h, followed by filtration. This procedure was repeated thrice before finally filtering and drying in vacuo to yield **6** in 45% yield. Anal. Calcd for $\text{C}_{10}\text{H}_{14}\text{O}_{11}\text{Na}_4\text{V} \cdot 2\text{H}_2\text{O}$: C, 24.54; H, 3.68; Na, 18.82; V, 10.42. Found: C, 24.87; H, 3.71; Na, 19.00; V, 10.66%.

$\text{Na}_4[\text{VO}(\text{-D-Ara})_2] \cdot \text{CH}_3\text{OH} \cdot 3\text{H}_2\text{O}$ (**7**). Compound **7** was synthesised and purified following the procedure given for **6**, except that 9:1 EtOH–acetone was used to precipitate a blue–green product **7** in 54% yield. Anal. Calcd for $\text{C}_{11}\text{H}_{18}\text{O}_{12}\text{Na}_4\text{V} \cdot 3\text{H}_2\text{O}$: C, 24.49; H, 4.45; Na, 17.07; V, 9.45. Found: C, 24.49; H, 4.54; Na, 17.14; V, 9.20%.

$\text{Ca}[\text{VO}(\text{-D-Gluconate})(\text{OCH}_3)_2] \cdot \text{H}_2\text{O}$ (**8**). To 25 mL methanolic solution of calcium gluconate (6.456 g, 15 mmol) was added NH_4VO_3 (0.589 g, 5 mmol) as a solid. An insoluble white suspension was noticed initially, and the reaction was stirred at room temperature for 3 days. The white residue was filtered using a Celite, and the filtrate was concentrated and precipitated with EtOH to give a green residue that was filtered and purified by adopting the procedure given for **6** to obtain **8** in 51% yield. Anal. Calcd. for $\text{C}_8\text{H}_{16}\text{O}_{10}\text{CaV} \cdot \text{H}_2\text{O}$: C, 25.19; H, 4.72; Ca, 10.50; V, 13.37. Found: C, 25.56; H, 4.60; Ca, 10.33; V, 13.51%.

$[\text{VO}(\text{-ascorbate})(\text{acac})] \cdot 0.25\text{MeOH}$ (**9**). To L-ascorbic acid (1.76 g, 10 mmol) in 50 mL of MeCN, was added $\text{VO}(\text{acac})_2$ (9.96 mmol, 2.65 g, solid), and the mixture was stirred for 24 h. The initial yellow colour of the solution slowly changed to green as the reaction proceeded. A precipitate that was obtained at the end of the reaction was separated by filtration. The residue was suspended in hot MeOH and stirred for 6 h to purify. This process was repeated thrice, whereupon a green solid complex **9** was obtained. The yield of this complex was calculated to be 60% based on vanadium. Anal. Calcd for $\text{C}_{11}\text{H}_{14}\text{O}_9\text{V} \cdot 0.25\text{CH}_3\text{OH}$: C, 38.69; H, 4.32; V, 14.61. Found: C, 38.93; H, 4.11; V, 15.08%.

Other oxovanadium–saccharide [13] complexes include the $\text{Na}_2[\text{VO}(\text{-D-Glc})_2] \cdot \text{CH}_3\text{OH}$ (VO–D–Glc, **10**), $\text{Na}_2[\text{VO}(\text{-D-Fru})_2]$ (VO–D–Fru, **11**), $\text{Na}_2[\text{VO}(\text{-D-Gal})_2] \cdot \text{CH}_3\text{OH}$, (VO–D–Gal, **12**), $\text{Na}_3[\text{VO}(\text{-D-Man})_2(\text{OCH}_3)] \cdot 4\text{CH}_3\text{OH}$ (VO–D–Man, **13**), and $\text{Na}_3[\text{VO}(\text{-D-Mal})_2] \cdot \text{CH}_3\text{OH}$, (VO–D–Mal, **14**).

Interaction of 1–4 and 10 with RNase and of 1 and 10 with DNase.—Each aliquot contained 0.001, 0.01 or 0.1 mol dm^{-3} of the vanadyl–saccharide complexes, **1–4** or **10**, 5 μL of RNA solution (83.35 $\mu\text{g}/5 \mu\text{L}$), 0.1 $\mu\text{g}/5 \mu\text{L}$ RNase (activity of 1 Kunitz units [15] per cm^3) and 10 μL of Hepes buffer (0.5 mol dm^{-3} Hepes buffer containing 1 mol dm^{-3} MgCl_2 , pH 7.5) and an appropriate amount of sterile water to make the solution up to 55 μL . RNase was preincubated with the complexes at 37 °C for 30 min and later added to the aliquot containing RNA and buffer. The reaction mixture containing all the above was incubated at 37 °C for 1 h. The reaction was quenched by the addition of 10 μL of dye (bromophenol blue in glycerol) to each aliquot. Agarose gel (1%) was prepared and run in 1X TBE (0.05 mol dm^{-3} Tris, 0.05 mol dm^{-3} boric acid, 0.001 mol dm^{-3} EDTA, pH 8.0) and electrophoresed at 200 V for 2 h. Ethidium bromide (0.5 $\mu\text{g}/\text{cm}^3$) was added to stain the gel for 30 min and later destained in distilled water, typically for 15–30 min. The gel was viewed under UV light at 302 nm, using a UV transilluminator and photographed on a polaroid film.

The interaction with DNase was carried out with 0.01 or 0.1 mol dm^{-3} of complexes **1** and **10**, which were added to 1 unit or 10 units of DNase and incubated at 37 °C for 30 min. This was later added to the aliquot containing 60 μM M13RF1 phage DNA. All other experimental conditions were essentially the same as above.

3. Results and discussion

All the saccharide complexes of vanadium are highly soluble in water, but insoluble in common organic solvents. Complexes **1–10** exhibited μ_{eff} values of 1.68–1.80 Bohr magnetons at room temperature corresponding to the spin-only magnetic moment of a d^1 configuration.

Absorption spectral studies.—(A) In solution: Complexes **1–9** in water showed two intra d -shell transitions, one in the region 640–690 nm (740 nm for **5** and 779 nm for **9**) with ε values in the range of 1–46 mol dm⁻³ cm⁻¹ and the other in the region

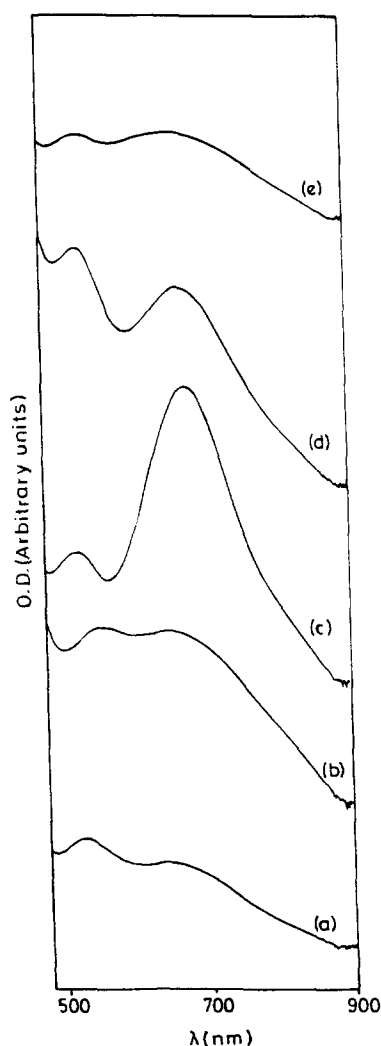


Fig. 1. Electronic absorption spectra in water for (a) **1**, (b) **2**, (c) **3**, (d) **7** and (e) **8** at ambient temperature.

Table 1

Absorption and reflectance spectral data of vanadyl–saccharide and saccharide derivative complexes **1–9** at ambient temperature

Complex	UV-vis: λ [nm] (ϵ [mol dm ⁻³ cm ⁻¹])
1 H ₂ O	650 (9); 535 (12); 330 (446); 260 (1931)
1 solid	655; 530
2 H ₂ O	640 (20); 560 (21); 395 (280); 280 (3041)
2 solid	640; 530
3 H ₂ O	674 (10); 522 (4); 420 (15); 360 (250)
3 solid	675; 520
4 H ₂ O	644 (9); 560 (8); 320 (20); 270 (125)
4 solid	630; 500
5 H ₂ O	740 (2); 533 (3); 330 (303); 265 (1910)
6 H ₂ O	650 (13); 535 (20); 280 (3040)
6 solid	660; 530
7 H ₂ O	668 (15); 525 (18); 320 (503); 265 (2413)
7 solid	675; 515
8 H ₂ O	653 (9); 533 (9); 390 (8); 310 (32); 270 (125)
8 solid	655; 530
9 H ₂ O	779 (46); 560 (42); 350 (70); 263 (170); 196 (640)
9 solid	765 (br), 565

520–590 nm with ϵ values in the range 1–42 mol dm⁻³ cm⁻¹ (Fig. 1, Table 1). Both the energy of these bands and their low ϵ values are indicative of $d \rightarrow d$ transitions and are attributable to ${}^2B_2 \rightarrow {}^2E$ and ${}^2B_2 \rightarrow {}^2B_1$ as explained by Ballhausen and Gray [16,17]. In many cases, the third $d \rightarrow d$ transition, ${}^2B_2 \rightarrow {}^2A_1$, is obscured by the intense charge-transfer transitions; however, in case of **3**, **8** and **9**, a shoulder is observed in the region 350–420 nm with ϵ values varying from 7 to 70 mol dm⁻³ cm⁻¹. Presence of this band above 333 nm is consistent with a 5-coordinated vanadyl species [17]. In case of **4** this is observed around 320 nm, indicating an axial coordination, which is explainable based on the composition. Removal of bound water at 180 °C is identified from TGA studies.

The presence of a fourth band in **8** at 310 nm ($\epsilon = 32$ mol dm⁻³ cm⁻¹) in water is surprising. In order to assess the origin of this band, absorption of **8** was carried out in a 9:1 Me₂SO–H₂O mixture, and the band was found to be shifted to 300 nm with an ϵ value of 215 mol dm⁻³ cm⁻¹. This may be due to the lifting of the degeneracy of the d_{xz} and d_{yz} (e) orbitals due to lower symmetry of the complex. Alternatively, this band can be explainable as a spin-forbidden charge-transfer transition. The latter seems to be a plausible explanation since the splitting of the 'e' level by as much as 6620 cm⁻¹ is rather unlikely. Low-symmetry oxovanadium complexes of tartrate, lactate, mandelate or malate groups have also shown four transitions between 10,000 and 26,000 cm⁻¹ as has been reported [18].

The absorption spectra of complex **9** recorded in water as a function of pH showed a shift from 746 nm (pH 1.05) to 880 nm (pH 11.6) with a progressive decrease in the intensity. A plot of band position as a function of pH is linear with a slope of about 12 nm/unit pH. However, no precipitation was seen in the entire pH range studied.

In water, complexes **1–9** showed two *d–d* bands in the CD spectrum similar to those found in the absorption spectra. Complexes of the type V_2L_2 (where L is a nucleoside) where L is bound as bidentate ligand through the 2', 3'-oxygen of the ribose unit are not CD active because the ligands are not chelating, but bind to two different metal centres [19]. Thus the CD response of complexes **1–9** is attributable to the chelating and bidentate nature of the saccharide ligands. Cyclic ester formation through chelation of nucleosides with vanadium giving complexes that are CD active has been reported [19].

(B) As a solid: The diffuse reflectance spectra of all the complexes in the solid state in the 400–900 nm range exhibited two well-defined transitions similar to those obtained in aqueous solution (Table 1). Thus the complexes seem to maintain their structural integrity both in the solution and in the solid states.

FTIR spectral studies.—FTIR spectra of all these compounds recorded in a KBr matrix were broad with the loss of fine structure otherwise found with the solid ligands. These results indicated an overall breakage of the hydrogen bonds present between the molecules in the free saccharides. Broad bands in the region 3389–3420 cm^{-1} with a shoulder at 3200 cm^{-1} are assignable to symmetric stretching of OH groups. The spectra showed a characteristic sharp band for $\nu_{\text{V=O}}$, mainly in the region 926–940 cm^{-1} for **1–4**, **6** and **7**. These vibrational frequencies are low as compared to vanadyl–hexose complexes [13] (945–960 cm^{-1}). The rather low $\nu_{\text{V=O}}$ values are attributable to intermolecular hydrogen bonds of the vanadyl group with the free hydroxyl groups and/or due to ion-pair interactions with Na^+ ions [20]. On the other hand, complex **9**, where no Na^+ is used, exhibits $\nu_{\text{V=O}}$ at 980 cm^{-1} , thus confirming our previous observations. The 700–1460 cm^{-1} region was usually dominated by the presence of deformation and bending modes of the CC, CO and CH_2 , and these were merged to give three to four broad bands indicating the presence of metal–saccharide interactions.

The vanadyl–inositol complex **5** exhibited spectra having sharper lines as compared to the other complexes reported here. The ν_{OH} region showed two components positioned at 3380 and 3230 cm^{-1} with a 2:1 intensity ratio, which is different from the others where the 3230 cm^{-1} is a weak shoulder. Changes were also noted in the $\nu_{\text{V=O}}$ region, where a sharp and intense band was observed at 900 cm^{-1} and a weak sharp shoulder at 950 cm^{-1} . The IR spectra in general seem to reflect the skeletal difference of the inositol from that of saccharides and their derivatives in these complexes. The area of the 1640 cm^{-1} band is strikingly low as compared to the others, indicating that the bound water content is low or absent. This is in accordance with the formula proposed without the presence of water molecule for **5** (see Experimental section).

In case of complex **9**, the ν_{OH} region was similar to that observed for the saccharide complexes. A strong and broad band at 1670 cm^{-1} with a shoulder at 1650 cm^{-1} was noticed in free ascorbic acid corresponding to the $\text{C}(1)=\text{O}$ and $\text{C}=\text{C}$ stretching vibrations. These were observed at 1673 cm^{-1} and 1645 cm^{-1} in **9**, clearly indicating that $\text{C}(1)=\text{O}$ is not involved in binding. This is in contrast to that observed for the Mn(II) , Zn(II) , Cd(II) and Hg(II) ascorbate complexes [21]. A broad band was observed at 1440 cm^{-1} corresponding to the $\text{C}(3)-\text{O}^-$ stretching vibrations as against that found at 1388 cm^{-1} in the free acid.

The saccharide acid complexes **4** and **8** showed strong bands at 1614 and 1607 cm^{-1}

and a weaker band at 1400 and 1403 cm^{-1} for the asymmetric and symmetric stretches, respectively, of the bound carboxylate ion. The $\nu_{\text{V=O}}$ in case of **8** is found at 954 cm^{-1} , a value higher than the other saccharide complexes.

Electrochemical studies.—All the complexes **1–9** exhibited an irreversible peak assignable to the V(IV) \rightarrow V(III) reduction in the cyclic voltammetric studies carried out in water at a hanging mercury drop electrode (HMDE) with the E_p^c values in the range -1.15 to -1.65 V at scan speed of 100 mV/s. Reduction of vanadyl complexes to the trivalent state entails loss of the vanadyl oxygen, and hence such reactions are usually irreversible [22]. The E_p^c (V) values are found in the order -1.65 (VO-D-Xyl), **2** > -1.64 (VO-Ino), **5** > -1.61 (VO-L-Sor), **3** > -1.60 (VO-D-Lyx), **6** ≥ -1.595 (VO-D-Ara), **7** > -1.56 (VO-D-GalA), **4** > -1.50 (VO-D-Rib), **1** > -1.245 (VO-D-Gluconate), and **8** > -1.15 (VO-L-Asc), **9**. The behaviour of E_p^c of these complexes is explainable based on the orientation of the hydroxyl groups. Ligands having at least one pair of hydroxyl groups in the cis position seem to prefer stabilizing V(IV) more and hence shows high cathodic reduction potential. Similar correlation was also made in case of VO-hexose complexes [13]. It is interesting to note that, while all the other ligands preferentially exist in cyclic forms, D-gluconate prefers a linear form possessing a carboxylic acid function. In general, the reduction potentials of the vanadyl-pentose complexes seems to be higher than that of their hexose counterparts [13].

Cyclic voltammograms of **1–14** have been recorded at HMDE at various pH values (1–12). The E_p^c values of all these complexes are sensitive to changes in pH, and the plots of E_p^c versus pH are linear. The slopes (mV/pH) from these plots are in the order as follows: **9** (120) $>$ **6** (76) $>$ **3** (72) $>$ **8** (70) $>$ **7** (67) $>$ **2** (65) $>$ **14** (63) $>$ **5** (60) $>$ **13** (50) $>$ **1** (47) $>$ **4** (37) $>$ **10** (33) $>$ **12** (25) $>$ **11** (20). Based on the values of the slope, the complexes can be divided into four categories: (i) those with a slope value of 120 mV per unit pH (**9**); (ii) those with a slope of 69 ± 9 mV per unit pH (**2**, **3**, **5–8** and **14**); (iii) those with a slope of 47–50 mV per unit pH (**1** and **13**); (iv) those with a slope of 27–37 mV per unit pH (**4**, **10–12**). The slope obtained for **9**, 120 mV/pH, is rather high. This is expected due to large changes occurring at the metal centre possessing one *acac* group, which can easily be hydrolysed from the metal centre in solution.

Addition of an appropriate amount of acid to a previously alkaline solution of the VO^{2+} -saccharide complex to bring the pH to the original value has given rise to identical voltammograms. No precipitation occurred in the entire pH range studied. These results indicate that the complexes are hydrolytically stable to the changes in the pH and that no disintegration of the compound occurs during the entire pH variation cycle. A CV of **1** recorded even after 60 days showed no change in the voltammograms and is indicative of the structural rigidity and stability of the complex in aqueous solution.

All the complexes **1–14** were studied for their oxidation behaviour at a Pt electrode in the pH range 2–9 and in the potential window of -0.5 and $+1.0$ V. None of the complexes gave any voltammetric response under these experimental conditions.

EPR studies.—The X-band EPR spectra of the vanadyl-saccharide complexes have been recorded at room temperature in both the solid state and in aqueous solution. The spectra recorded in solution at room temperature gave an eight-line pattern ($I = 7/2$)

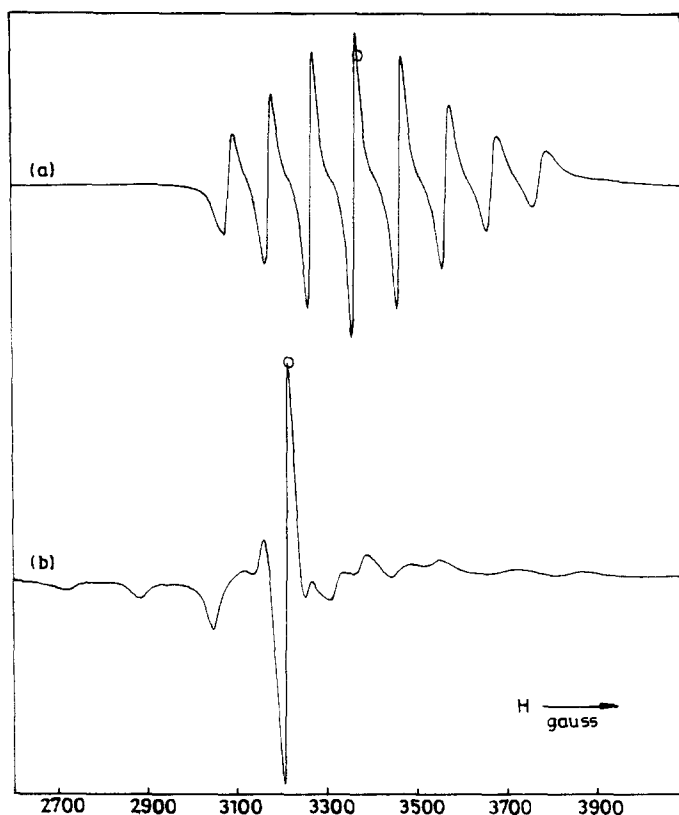


Fig. 2. EPR spectra of complex **1** in water at (a) room temperature and (b) liquid N_2 temperature. The circle indicates the TCNE marker ($g \approx 2.00277$).

with an isotropic behaviour and are identical to those observed as in the case of the vanadyl–hexose complexes [13]. EPR of these complexes recorded in water at liq N_2 temperature display anisotropy. Representative spectra of complex **1** are shown in Fig. 2. The hyperfine parameters are derived directly from the spectrum by graphical methods based on peak assignments (Table 2). The hyperfine splitting parameters are indicative of the presence of VO^{2+} unit in $VO(O)_4$ environment [23]. The $g_{\parallel} < g_{\perp}$ and $A_{\parallel} > A_{\perp}$ relationships are characteristic of an axially compressed d_{xy}^1 configuration [24]. This is typical of pentacoordinated V(IV)O complexes. Room temperature EPR spectra of complexes **1–4** and **10** recorded in Hepes buffer (pH 7.50) were identical with those observed in water. The EPR spectrum of complex **8** also showed an isotropic, eight-line pattern in water at room temperature that is characteristic of a VO^{2+} ion. This indicates that the precursor V(V) species is reduced and further complexed during the reaction with gluconate.

Correlations of the ESR parameters such as g_0 versus A_0 and g_{\parallel} versus A_{\parallel} have been employed for analyzing the coordination of the vanadium centre, especially in case of naturally occurring vanadium(IV) compounds by Sakurai and others [23]. Cores like

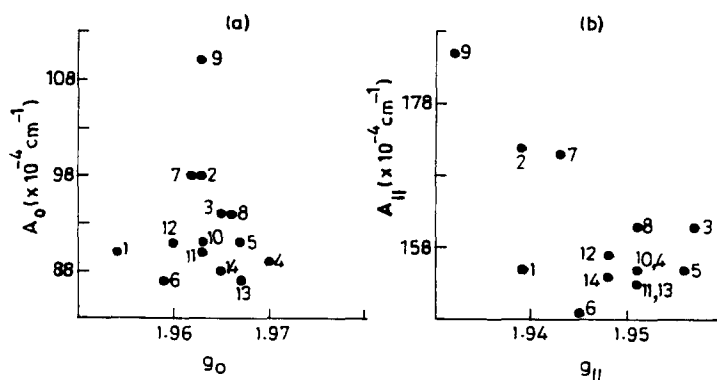
Table 2

Hyperfine coupling parameters in water for vanadyl–saccharide complexes **1–14** at liq N₂ temperature

Complex	g_0	g_{\parallel}	g_{\perp}	A_0	A_{\parallel} (10^{-4} cm ⁻¹)	A_{\perp} (10^{-4} cm ⁻¹)
1	1.954	1.939	1.961	90.2	155.3	57.7
2	1.963	1.939	1.975	97.7	171.1	61.4
3	1.965	1.957	1.969	93.9	160.9	59.5
4	1.970	1.951	1.980	89.3	155.3	56.7
5	1.967	1.956	1.974	91.1	155.3	59.5
6	1.959	1.945	1.966	87.4	149.7	56.7
7	1.962	1.943	1.972	97.7	170.2	61.4
8	1.966	1.951	1.974	93.9	160.9	59.5
9	1.963	1.932	1.978	108.8	183.2	72.5
10	1.963	1.951	1.969	91.1	155.3	59.5
11	1.963	1.951	1.969	90.2	153.5	59.5
12	1.960	1.948	1.966	91.1	157.2	58.6
13	1.967	1.951	1.976	87.4	153.5	53.9
14	1.965	1.948	1.974	88.4	154.4	54.9

VO(O)₄, VO(O₂O₂⁻), VO(O₂N₂), VO(N₄), VO(O₂S₂), VO(N₂S₂) and VO(S₄) occupy various zones on the g_{\parallel} versus A_{\parallel} plots. Most of the VO(O)₄ in their plot seem to aggregate between A_{\parallel} values of 167–186 ($\times 10^{-4}$ cm⁻¹) and g_{\parallel} values of 1.93–1.94. It is interesting to note that though the vanadyl–saccharide complexes reported here are VO(O)₄ in nature, the values of A_{\parallel} and g_{\parallel} are in the range of 149–186 ($\times 10^{-4}$ cm⁻¹) and 1.93–1.96, respectively (Fig. 3).

EPR spectra recorded as a function of pH 1–9 for complex **1** indicate its structural rigidity and stability. ρ^d [where $\rho^d = 3d$ spin density; $= (7/6P)(A_{\parallel} - A_{\perp})$ and P is the dipolar coupling parameter and is equal to 127.4×10^{-4} cm⁻¹] [17,25] values at different pH showed an increasing charge occupancy around the metal centre with the plot of ρ^d versus pH being linear (Fig. 4a). This has also been confirmed by cyclic voltammetry where the plot of ρ^d versus E_p^c is linear (Fig. 4b), indicating that increasing the charge at the metal centre would make it more difficult to reduce.

Fig. 3. (a) g_0 versus A_0 ; (b) g_{\parallel} versus A_{\parallel} for the VO²⁺–saccharides.

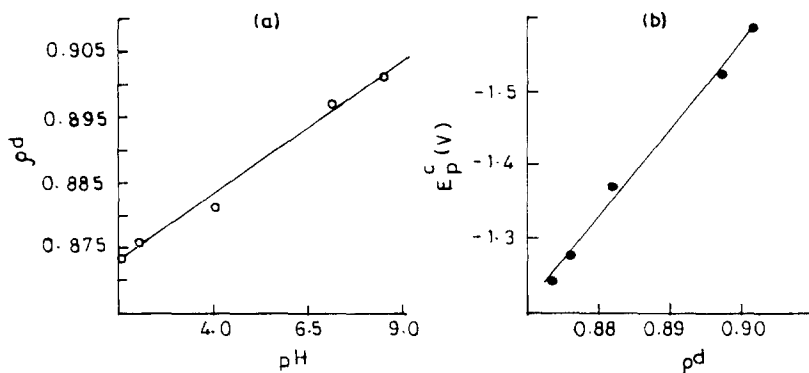


Fig. 4. (a) ρ^d versus pH; (b) ρ^d versus E_p° for complex 1.

EPR spectra recorded at different pH values for an aqueous solution of complex **9** at room temperature exhibited isotropic spectra under acidic conditions and became featureless at $\text{pH} > 9$. This is indicative that the vanadium centre is either oxidised to V(V) or forms another species with magnetically coupled V(IV) centres that are EPR silent. Addition of concentrated HCl to the previously alkaline solution of this complex to bring the pH to 1.24 showed once again an isotropic EPR behaviour. Thus the present studies provided evidence for the reversibility of these two forms and also the robust nature of the complex in the range of pH 1–13. As in case of hexose–vanadyl complexes [13], all the complexes reported herein were also found to be stable towards aerial oxidation in aqueous solution for a period of 8 weeks, based on EPR and absorption studies.

Nature of the products.—There exists considerable interest in vanadium alkoxides and oxohydroxy species [26]. Although the importance of vanadium–saccharide complexes has been identified, relatively less is known, particularly due to the lack of synthetic strategies to make low molecular weight, soluble and characterizable complexes. The VO^{2+} –saccharide and related complexes reported here except **9** are found to be anionic with Na^+ as the counter cation (Ca^{2+} in case of **8**). Although complexation between saccharides and vanadyl ion was proposed by others [27], ours is the first case of isolation and characterization of the solid products [13]. ^1H NMR spectra of all these complexes showed line broadening indicative of the presence of a paramagnetic metal centre, and hence could not be used effectively to identify the skeletal protons. However, in case of complex **9**, the protons of the acetylacetonato moiety could be identified. Spectra of complexes **2** and **8** showed peaks corresponding to $-\text{OCH}_3$ at 3.33 and 3.62 ppm, respectively. While the presence of the oxovanadium(IV) moiety is shown in all the complexes based on absorption and EPR studies, FTIR studies support the presence of $\text{V}=\text{O}$, and circular dichroism studies reveal that the ligands are bidentate and chelating. The identification of metal–saccharide complex formation was further supported by FTIR studies. The ligands used in the present study seem to preferably bind to the V(IV) centre in all cases including that of **8**, where the precursor V(V) is reduced to V(IV) and is further complexed.

The solution stability of these complexes is shown by UV-vis absorption, cyclic voltammetry and EPR studies. Meaningful correlations have been drawn between the data for all the vanadyl–saccharide complexes. Plots A_{\parallel} versus g_{\parallel} have shown that for a set of VO(O) complexes the range can be extended between 149–186 ($\times 10^{-4} \text{ cm}^{-1}$) and 1.93–1.96. Such information might help in unravelling the nature of ligands bound to naturally occurring vanadyl species.

While the RT magnetic moments are indicative of a d^1 system, EPR spectra are devoid of any vanadyl dimers with low lying triplet states in the present set of complexes. Vanadyl dimers with low lying triplet states show a well-resolved isotropic spectrum comprised of 15 lines. Such dimers also show a weak transition at $g \sim 4$ as a result of ‘forbidden’ $\Delta M_s = \pm 2$ triplet–singlet transitions [28]. Various efforts to obtain single crystals of X-ray quality of these complexes have not been successful. In the reduction of Cr(VI) using saccharides and their derivatives to form Cr(III)–saccharide complexes, the presence of OH on C-2 of the saccharide chain was found to be important, supporting the coordination of C-2–O[−] [11,12]. EXAFS studies in the case of Fe–saccharide complexes suggested that the saccharide ligands act as bidentate and chelating [29]. Based on the coordination mode of saccharides towards, inter alia, Cr(III) [11], Fe(III) [29] and V(V) [10] and on various studies reported here including those of observed analytical results, we suggest the following formulae for the VO²⁺–saccharide complexes: Na₄[VO-(D-Rib)₂] · H₂O for **1**, Na₂[VO-(D-Xyl)₂] · CH₃OH for **2**, Na₄[VO-(L-Sor)₂] · 3H₂O for **3**, Na₂[VO-(D-GalA)(H₂O)] for **4**, Na₂[VO-(Ino)₂] for **5**, Na₄[VO-(D-Lyx)₂] · 2H₂O for **6**, Na₄[VO-(D-Ara)₂] · CH₃OH · 3H₂O for **7**, Ca[VO-(D-GlcA)(OCH₃)₂] · H₂O for **8** and [VO-(L-Asc)(acac)] · 0.25 CH₃OH for **9**. The schematic representation of complexes **2** and **10** are shown in Fig. 5.

In vitro interaction of **1–4** and **10** with RNase and **1**, **10** with DNase.—Rehder’s group expressed that V(V) strives for a trigonal bipyramidal geometry in the presence of alkoxo ligands, thereby making the alkoxo oxovanadium complexes as transition-state

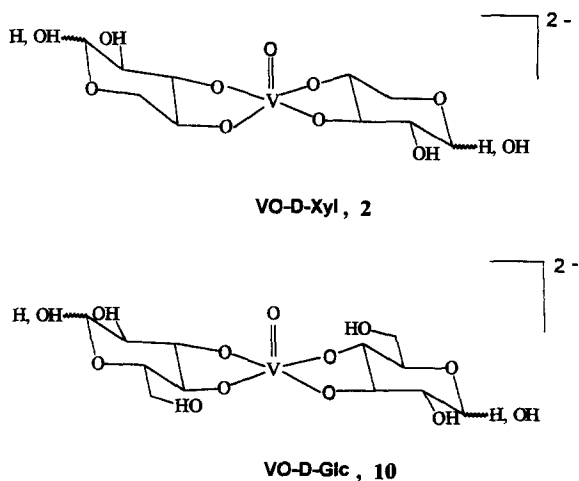


Fig. 5. Schematic representation of complexes **2** and **10**.

analogues [30] for enzymes catalyzing reactions that involve a pentacoordinate trigonal bipyramidal (*thp*) phosphorous centre. However, the favoured geometry for crystalline complexes of oxovanadium(IV and V) appear to be square-pyramidal ones, though some possess *thp* geometry [20,31–33]. A very relevant study of the in vitro interaction of the vanadyl–saccharide complexes with RNase and DNase has been carried out using **1**–**4** and **10**. While on one hand V imitates P in biological systems, it is the former that can form complexes with coordination number greater than 4 with redox activity. The vanadyl–ribonucleoside complex (VRC) mixture was found to inhibit RNase activity [9], but the products of the reaction mixture were neither isolated nor characterized and were further shown to contain Na_2SO_4 as an impurity. A vanadate–uridine RNase system has been well characterized by X-ray and neutron diffraction methods and established the distorted *thp* arrangement around the vanadium centre [34]. Using the rationale that oxovanadium can act as a transition-state analogue by binding to the sugar oxygens in the nucleosides to form a *thp* geometry, the effect of vanadyl–saccharide complexes towards RNase and DNase activity has been studied using agarose gel electrophoresis.

RNase was preincubated with different concentrations of the complexes as indicated in the experimental section. This was later incubated with RNA for 1 h. The complexes (at $0.1 \text{ mol dm}^{-3} \text{ cm}^{-1}$) were also incubated with RNA and used as a control. Increasing amounts of RNA were detected on the gel with increasing concentrations of complexes **1**, **2**, **4** and **10**. This indicates that these complexes showed considerable inhibition of the RNase activity ($\mathbf{1} > \mathbf{10} \geq \mathbf{2} \sim \mathbf{4}$). However, complex **3**, which is derived from L-sorbose, showed no inhibitory effect on RNase activity. The controls in the same experiment lacking the complexes clearly showed no such protection, and the RNA was degraded by RNase. The inhibition profile of complexes **1** and **10** as a function of concentration is shown as a histogram in Fig. 6. These studies suggest that while the geometry at the metal centre influences its biological response, the stereochemistry of the ligands also effects in the overall activity.

When complexes **1** and **10** were incubated with DNase under similar experimental conditions, no such protection on DNA was observed. Although there are many similarities between RNases and DNases, a clear mechanistic distinction is that the cyclic 2',3'-phosphate cannot form an intermediate during DNase-mediated hydrolysis due to the lack of a 2'-OH group [35]. Further, the cyclic phosphate ester formed in the RNase-mediated hydrolysis of RNA (Fig. 7a) structurally resembles the vanadyl–saccharide complex as shown for **1** in Fig. 7b. All this suggests that some of the

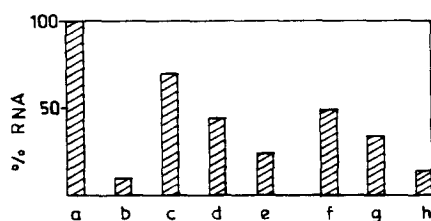


Fig. 6. RNase inhibition profile of complexes **1** and **10** as a function of concentration. (a) RNA; (b) RNA + RNase; (c) (b) + **1** (0.1 mol dm^{-3}); (d) (b) + **1** (0.01 mol dm^{-3}); (e) (b) + **1** ($0.001 \text{ mol dm}^{-3}$). (f), (g) and (h) are the same as (c), (d) and (e) except that complex **10** was used in place of **1**.

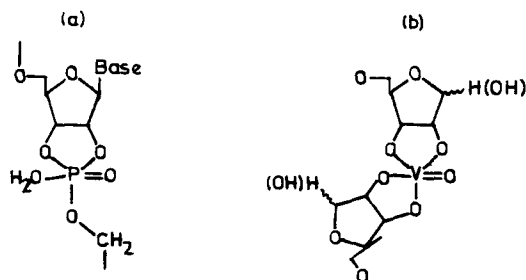


Fig. 7. (a) Transition-state complex in the RNase-catalysed hydrolysis of RNA, and (b) proposed schematic representation of complex 1.

vanadyl–saccharide complexes can act as substrate analogues to the enzyme RNase. Also these complexes did not show any effect on the RNA alone. This is an important aspect if these complexes were to be used in the *in vivo* isolation of mRNA from cells. As the RNase inhibiting activity of **1** is about 70% under the present experimental conditions, it may be possible to enhance this activity through extensive experimentation so that it can be used in RNA isolation studies. Since the RNase enzyme cleaves the RNA in two distinct steps, understanding the actual step of inhibition by these complexes, site of their interaction and also the inability of complex **3** for such inhibition will be a part of our continuing research pursuit.

Acknowledgements

A.S. thanks the Department of Atomic Energy, India for the award of a Dr. K.S. Krishnan research fellowship. C.P.R. acknowledges the Department of Science and Technology, New Delhi, for financial support. The BAS100B instrument was purchased from DST funds. RSIC, IIT, Bombay, is thanked for recording the EPR spectra and performing the ICP-AES analyses. We thank Mr. G. Karthikeyan and Ms. R. Anuradha of the Molecular Biology Unit, Prof. S. Mitra and Mr. B. Kansara, Chemical Physics Group, TIFR, Bombay for some experimental help.

References

- [1] M. Riediker and R.O. Duthaler, *Angew. Chem., Int. Ed. Engl.*, 28 (1989) 494–495; R.O. Duthaler, P. Herold, W. Lottenbach, and K. Oertle, *Angew. Chem., Int. Ed. Engl.*, 28 (1989) 495–497; G. Bold, R.O. Duthaler, and M. Riediker, *Angew. Chem., Int. Ed. Engl.*, 28 (1989) 497–498; D.M. Whitfield, S. Stojkovsky, and B. Sarkar, *Coord. Chem. Rev.*, 122 (1993) 171–225.
- [2] L. Josephson and L.C. Cantley, Jr., *Biochemistry*, 16 (1977) 4572–4578.
- [3] D. Rehder, *Angew. Chem., Int. Ed. Engl.*, 30 (1991) 148–167; R. Wever, in R.B. King (Ed.), *Encyclopedia of Inorganic Chemistry*, Vol. 8, Wiley, New York, 1994, pp 4296–4304; N.D. Chasteen (Ed.), *Vanadium in Biological Systems*, Kluwer, Netherlands, 1990.
- [4] H. Michibata, T. Miyamoto, and H. Sakurai, *Biochem. Biophys. Res. Commun.*, 141 (1986) 251–257; H. Michibata, J. Hirata, T. Terada, and H. Sakurai, *Experientia*, 44 (1988) 906–907.

- [5] Y. Shechter, *Diabetes*, 39 (1990) 1–5.
- [6] B.I. Posner, R. Faure, J.W. Burgess, A.P. Bevan, D. Lachance, G. Zhang-Sun, I.G. Fantus, J.B. Ng, D.A. Hall, B.S. Lum, and A. Shaver, *J. Biol. Chem.*, 269 (1994) 4596–4604; A. Shaver, J.B. Ng, D.A. Hall, B.S. Lum, and B.I. Posner, *Inorg. Chem.*, 32 (1993) 3109–3113.
- [7] J.H. McNeill, V.G. Yuen, H.R. Hoveyda, and C. Orvig, *J. Med. Chem.*, 35 (1992) 1489–1491.
- [8] H. Watanabe, M. Nakai, K. Komazawa, and H. Sakurai, *J. Med. Chem.*, 37 (1994) 876–877.
- [9] S.L. Berger and C.S. Birkenmeier, *Biochemistry*, 18 (1979) 5143–5149.
- [10] S.J. Angus-Dunne, R.J. Batchelor, A.S. Tracey, and F.W.B. Einstein, *J. Am. Chem. Soc.*, 117 (1995) 5292–5296.
- [11] C.P. Rao, S.P. Kaiwar, and M.S.S. Raghavan, *Polyhedron*, 13 (1994) 1895–1906; S.P. Kaiwar, M.S.S. Raghavan, and C.P. Rao, *J. Chem. Soc., Dalton Trans.*, (1995) 1569–1576.
- [12] K. Geetha, M.S.S. Raghavan, S.K. Kulshreshtha, R. Sasikala, and C.P. Rao, *Carbohydr. Res.*, 271 (1995) 163–175; S.P. Kaiwar and C.P. Rao, *Chem. Biol. Interact.*, 95 (1995) 89–96; R.P. Bandwar, M. Giralt, J. Hidalgo, and C.P. Rao, *Carbohydr. Res.*, 284 (1996) 73–84.
- [13] A. Sreedhara, M.S.S. Raghavan, and C.P. Rao, *Carbohydr. Res.*, 264 (1994) 227–235.
- [14] J. Sambrook, E.F. Fritsch, and T. Maniatis, *Molecular Cloning, A Laboratory Manual*, Vol. 1, Cold Spring Harbor Laboratory Press, 1989.
- [15] M. Kunitz, *J. Biol. Chem.*, 164 (1946) 563–568.
- [16] C.J. Ballhausen and H.B. Gray, *Inorg. Chem.*, 1 (1962) 111–116.
- [17] R. Deeth, *J. Chem. Soc., Dalton Trans.*, (1991) 1467–1477.
- [18] J. Selbin and L. Morpurgo, *J. Inorg. Nucl. Chem.*, 27 (1965) 673–678.
- [19] D.C. Crans, S.E. Harnung, E. Larsen, P.K. Shin, L.A. Theisen, and I. Trabjerg, *Acta Chem. Scand.*, 45 (1991) 456–462.
- [20] G. Asgedom, A. Sreedhara, J. Kivikoski, J. Valkonen, and C.P. Rao, *J. Chem. Soc., Dalton Trans.*, (1995) 2549–2466.
- [21] H.A. Tajmir-Riahi, *J. Inorg. Biochem.*, 42 (1991) 47–55.
- [22] J. Selbin, *Chem. Rev.*, 65 (1965) 153–175; S.R. Cooper, Y.B. Koh, and K.N. Raymond, *J. Am. Chem. Soc.*, 104 (1982) 5092–5102.
- [23] H. Sakurai, J. Hirata, and H. Michibata, *Inorg. Chim. Acta*, 152 (1988) 177–180.
- [24] M. Branca, G. Micera, A. Dessi, D. Sanna, and K. Raymond, *Inorg. Chem.*, 29 (1990) 1586–1589.
- [25] A.L. Rieger, J.L. Scott, and P.H. Rieger, *Inorg. Chem.*, 33 (1994) 621–622.
- [26] D.C. Crans, H. Chen, and R.A. Felty, *J. Am. Chem. Soc.*, 114 (1992) 4543–4550; D.C. Crans, R.A. Felty, O.P. Anderson, and M.M. Miller, *Inorg. Chem.*, 32 (1993) 247–248; P.J. Toscano, E.J. Schermerhorn, C. Dettelbacher, D. Macherone, and J. Zubietta, *J. Chem. Soc., Chem. Commun.*, (1991) 933–934.
- [27] M. Branca, G. Micera, A. Dessi, and D. Sanna, *J. Inorg. Biochem.*, 45 (1992) 169–177.
- [28] C.W. Hahn, P.G. Rasmussen, and J.C. Bayon, *Inorg. Chem.*, 31 (1992) 1963–1965.
- [29] L. Nagy, H. Ohtaki, H. Yamaguchi, and M. Nomura, *Inorg. Chim. Acta*, 159 (1989) 201–207.
- [30] F. Hillerms, F. Olbrich, U. Behrens, and D. Rehder, *Angew. Chem., Int. Ed. Engl.*, 31 (1992) 447–448; J. Ritcher and D. Rehder, *Z. Naturforsch.*, B, 46 (1991) 1613–1520.
- [31] R.N. Lindquist, J.L. Lynn, Jr., and G.E. Lienhard, *J. Am. Chem. Soc.*, 95 (1973) 8762–8768.
- [32] G. Asgedom, A. Sreedhara, J. Kivikoski, E. Kolehmainen, and C.P. Rao, *J. Chem. Soc., Dalton Trans.*, (1996) 93–97.
- [33] L.M. Mokry and C.J. Carrano, *Inorg. Chem.*, 32 (1993) 6119–6121.
- [34] B. Borah, C.-W. Chen, W. Egan, M. Miller, A. Wlodawer, and J.S. Cohen, *Biochemistry*, 24 (1985) 2058–2067.
- [35] C. Walsh, *Enzymatic Reaction Mechanisms*, W.H. Freeman and Co., 1979.